Controlling the Cellular Uptake of Gold Nanorods

Terry B. Huff,† Matthew N. Hansen,† Yan Zhao,† Ji-Xin Cheng,*,†,‡ and Alexander Wei*,†

Department of Chemistry and Weldon School of Biomedical Engineering, Purdue University, West Lafayette, Indiana 47907

Received September 8, 2006. In Final Form: November 21, 2006

Gold nanorods coated with cetyltrimethylammonium bromide (CTAB), a cationic micellar surfactant used in nanorod synthesis, were rapidly and irreversibly internalized by KB cells via a nonspecific uptake mechanism. Internalized nanorods near the cell surface were monitored by two-photon luminescence (TPL) microscopy and observed to migrate toward the nucleus with a quadratic rate of diffusion. The internalized nanorods were not excreted but formed permanent aggregates within the cells, which remained healthy and grew to confluence over a 5-day period. Nonspecific nanorod uptake could be greatly reduced by displacing the CTAB surfactant layer with chemisorptive surfactants, particularly by the conjugation of poly(ethylene glycol) chains onto nanorods using in situ dithiocarbamate formation.

Introduction

Recent advances in the synthesis and physical characterization of plasmon-resonant nanoparticles have set the stage for their application toward biomedical imaging and image-guided therapies. Numerous studies have established their use as optical contrast agents for in vitro imaging of tissue sections or cell cultures[1] and, more recently, for in vivo imaging with live animal models.[2] Plasmon-resonant nanoparticles also have the capacity to convert light energy into heat when irradiated at low power,[3] suggesting possibilities for noninvasive therapies based on spatially localized or cell-selective hyperthermia.[4−6] For in vivo applications, the window of highest optical transmittivity through biological tissues lies in the near-infrared (NIR) spectral range,[7] and current efforts are focused on anisotropic gold nanoparticles whose optical resonances have been tuned to wavelengths above 750 nm. Examples of NIR-active contrast agents used to enhance biological imaging modalities include gold nanoshells,[6,8] nanoparticle-coated microspheres,[9] hollow gold nanocubes,[10] and gold nanorods.[2,5,11] The latter are especially appealing as NIR-active imaging agents because they support a higher absorption cross section per unit volume than other types of nanoparticles, and their longitudinal plasmon resonances (LPRs) can be tuned as a function of aspect ratio.[12]

Although the use of nanoengineered particles for biomedical applications is very promising, all such materials are subject to a preclinical evaluation process commonly referred to as adsorption, distribution, metabolism, excretion, and toxicity (ADMET) profiling. The factors which determine the ADMET profiles of nanoparticles are not yet well-defined, stimulating much discussion and research in this area.[13] For example, while it is widely assumed that colloidal gold particles are biologically inert, there is a remarkable variance in the cytotoxicity and uptake of gold nanoparticles with respect to surfactant coating, size, and shape.[14−17] Other aspects of nanoparticle delivery such as cell specificity, reversibility of accumulation, and mechanism of uptake also require proper characterization prior to deployment in a clinical setting.

Here, we identify and characterize the nonspecific cell uptake of gold nanorods coated with cetyltrimethylammonium bromide (CTAB), a cationic micellar surfactant. Gold nanorods are typically prepared in the presence of micelle-forming detergents such as CTAB,[18−20] which also helps to maintain the nanorods

* Corresponding authors. E-mail: jcheng@purdue.edu, alexwei@purdue.edu.

† Department of Chemistry.

‡ Weldon School of Biomedical Engineering.

(1) Recent examples: (a) Xu, X.-H. N.; Chen, J.; Jeffers, R. B.; Kyriacou, S. *Nano Lett.* **2002**, *2*, 175−182. (b) Sokolov, K.; Follen, M.; Aaron, J.; Pavlova, I.; Malpica, A.; Lotan, R.; Richards-Kortum, R. *Cancer Res.* **2003**, *63*, 1999−2004. (c) Yelin, D.; Oron, D.; Thiberge, S.; Moses, E.; Silberberg, Y. *Opt. Express* **2003**, *11*, 1385−1391. (d) Zhao, Y.; Sadtler, B.; Min, L.; Hockerman, G. H.; Wei, A. *Chem. Commun.* **2004**, 784−785. (e) Copland, J. A.; Eghtedari, M.; Popov, V. L.; Kotov, N.; Mamedova, N.; Motamedi, M.; Oraevsky, A. A. *Mol. Imaging Biol.* **2004**, *6*, 341−349. (f) El-Sayed, I. H.; Huang, X.; El-Sayed, M. A. *Nano Lett.* **2005**, *5*, 829−834.

(2) Wang, H.; Huff, T. B.; Zweifel, D. A.; He, W.; Low, P. S.; Wei, A.; Cheng, J.-X. *Proc. Natl. Acad. Sci. U.S.A.* **2005**, *102*, 15752−15756.

(3) Chou, C.-H.; Chen, C.-D.; Wang, C. R. C. *J. Phys. Chem. B* **2005**, *109*, 11135−11138.

(4) (a) Pitsillides, C. M.; Joe, E. K.; Wei, X.; Anderson, R. R.; Lin, C. P. *Biophys. J.* **2003**, *84*, 4023−4032. (b) Zharov, V. P.; Mercer, K. E.; Galitovskaya, E. N.; Smeltzer, M. S. *Biophys. J.* **2005**, *90*, 619−627.

(5) Huang, X.; El-Sayed, I. H.; Qian, W.; El-Sayed, M. A. *J. Am. Chem. Soc.* **2006**, *128*, 2115−2120.

(6) (a) Hirsch, L. R.; Stafford, R. J.; Bankson, J. A.; Sershen, S. R.; Rivera, B.; Price, R. E.; Hazle, J. D.; Halas, N. J.; West, J. L. *Proc. Natl. Acad. Sci. U.S.A.* **2003**, *100*, 13549−13554. (b) O'Neal, D. P.; Hirsch, L. R.; Halas, N. J.; Payne, J. D.; West, J. L. *Cancer Lett.* **2004**, *209*, 171−176.

(7) Helmchen, F.; Denk, W. *Nat. Methods* **2005**, *2*, 932−940.

(8) (a) Wu, C. F.; Liang, X. P.; Jiang, H. B. *Opt. Commun.* **2005**, *253*, 214−221. (b) Loo, C.; Lowery, A.; West, J.; Halas, N.; Drezek, R. *Nano Lett.* **2005**, *5*, 709−711. (c) Liu, Z. X.; Song, H. W.; Yu, L. X.; Yang, L. M. *Appl. Phys. Lett.* **2005**, *86*, 113109.

(9) Lee, T. M.; Oldenburg, A. L.; Sitafalwalla, S.; Marks, D. L.; Luo, W.; Toublan, F. J.-J.; Suslick, K. S.; Boppart, S. A. *Opt. Lett.* **2003**, *28*, 1546−1548.

(10) Chen, J.; Saeki, F.; Wiley, B. J.; Cang, H.; Cobb, M. J.; Li, Z.-Y.; Au, L.; Zhang, H.; Kimmey, M. B.; Li, X.; Xia, Y. *Nano Lett.* **2005**, *5*, 473−477.

(11) (a) Oldenburg, A.; Zweifel, D. A.; Xu, C.; Wei, A.; Boppart, S. A. *Proc. SPIE Int. Soc. Opt. Eng.* **2005**, *5703*, 50−60. (b) Oldenburg, A. L.; Hansen, M. H.; Zweifel, D. A.; Wei, A.; Boppart, S. A. *Opt. Express* **2006**, *14*, 6724−6738.

(12) (a) Burda, C.; Chen, X.; Narayanan, R.; El-Sayed, M. A. *Chem. Rev.* **2005**, *105*, 1025−1102. (b) Wei, A. In *Nanoparticles: Scaffolds and Building Blocks*; Rotello, V. M., Ed.; Kluwer Academic: New York, 2004; pp 173−200. (c) Pérez-Juste, J.; Pastoriza-Santos, I.; Liz-Marzán, L. M.; Mulvaney, P. *Coord. Chem. Rev.* **2005**, *249*, 1870−1901.

(13) (a) Balshaw, D. M.; Philbert, M.; Suk, W. A. *Toxicol. Sci.* **2005**, *88*, 298−306. (b) Singh, R.; Pantarotto, D.; Lacerda, L.; Pastorin, G.; Klumpp, C. P. M.; Bianco, A.; Kostarelos, K. *Proc. Natl. Acad. Sci. U.S.A.* **2006**, *103*, 3357−3362.

(14) (a) Goodman, C. M.; McCusker, C. D.; Yilmaz, T.; Rotello, V. M. *Bioconjugate Chem.* **2004**, *15*, 897−900. (b) Shukla, R.; Bansal, V.; Chaudhary, M.; Basu, A.; Bhonde, R. R.; Sastry, M. *Langmuir* **2005**, *21*, 10644−10654.

(15) Connor, E. E.; Mwamuka, J.; Gole, A.; Murphy, C. J.; Wyatt, M. D. *Small* **2005**, *1*, 325−327.

(16) Takahashi, H.; Niidome, Y.; Niidome, T.; Kaneko, K.; Kawasaki, H.; Yamada, H. *Langmuir* **2006**, *22*, 2−5.

(17) Chithrani, B. D.; Ghazani, A. A.; Chan, W. C. W. *Nano Lett.* **2006**, *6*, 662−668.

(18) (a) Yu, Y.-Y.; Chang, S.-S.; Lee, C.-L.; Wang, C. R. C. *J. Phys. Chem. B* **1997**, *101*, 6661−6664. (b) Chang, S.-S.; Shih, C.-W.; Chen, C.-D.; Lai, W.-C.; Wang, C. R. C. *Langmuir* **1999**, *15*, 701−709. (c) Kim, F.; Song, J. H.; Yang, P. *J. Am. Chem. Soc.* **2002**, *124*, 14316−14317. (d) Niidome, T.; Nishioka, K.; Kawasaki, H.; Yamada, H. *Chem. Commun.* **2003**, 2376−2377. (e) Jana, N. R.; Gearheart, L.; Murphy, C. J. *Adv. Mater.* **2001**, *13*, 1389−1393. (f) Nikoobakht, B.; El-Sayed, M. A. *Chem. Mater.* **2003**, *15*, 1957−1962.

10.1021/la062642r CCC: $37.00 © 2007 American Chemical Society
Published on Web 01/09/2007

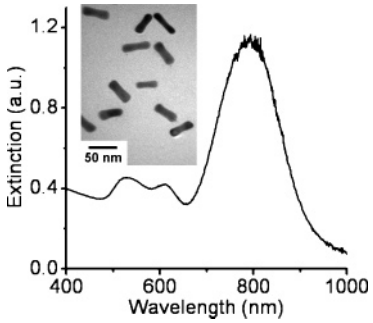

Figure 1. Extinction profile of Au nanorods ($\lambda_{LPR} = 795$ nm). The short wavelength peak ($\lambda \approx 520$ nm) is from the nanorods' transverse plasmon mode; the intermediate peak ($\lambda \approx 610$ nm) is produced by a small percentage of non-rodlike nanoparticles. Inset: TEM image of nanorods (JEOL 2000FX, 200 kV).

Scheme 1. Conjugation of mPEG Chains ($n \approx 75$) onto Nanorod Surfaces by in situ DTC Formation

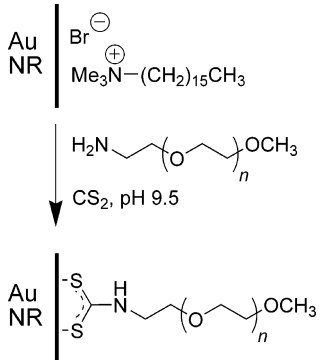

as stable dispersions in aqueous solution if kept above their critical micelle concentration (ca. 1 mM).[21] The high concentration of CTAB employed in nanorod synthesis has raised some concerns regarding their toxicity.[22] Recent studies have shown that CTAB-coated gold nanoparticles by themselves have minimal in vitro cytotoxicity if the surfactant concentration is reduced;[15,16] nevertheless, downstream effects of nonspecific nanorod uptake are also of concern for reasons outlined above.[13] We provide a practical solution to this issue by displacing the CTAB coating with chemisorptive polyethylene glycol chains based on in situ dithiocarbamate formation, a recently introduced method for metal surface functionalization.[23]

Experimental Methods

CTAB-coated nanorods were prepared in high yields using the seeded-growth conditions described by Sau and Murphy[19] and treated with sodium sulfide to arrest further growth and subsequent changes in LPR.[20] These sulfide-treated nanorods possess a dumbbell-like geometry with flared ends and produce a strong, stable LPR in the NIR region ($\lambda = 795$ nm; see Figure 1). The nanorod dispersions were centrifuged and redispersed in deionized water two times (24 000 *g*, 5 min per cycle) with a final optical density in the range 1.0−1.2.

Methylated poly(ethylene glycol) chains bearing a terminal amine (mPEG-NH_2, Nektar) were conjugated onto nanorods by in situ dithiocarbamate (DTC) formation (Scheme 1).[23] In a typical procedure, a 3-mL suspension of CTAB-coated nanorods was treated with a mixed-bed ion-exchange resin (Amberlite MB-3, Sigma) at room temperature overnight to further reduce unassociated surfactant and other ions,[24] then decanted and treated while stirring with 0.5 mL of a 2% aqueous solution of mPEG-NH_2 adjusted to pH 9.5, followed by dropwise addition of 0.5 mL of a saturated (28 mM) aqueous solution of freshly distilled CS_2. The mixture was stirred for 12 h, then subjected to membrane dialysis for 12 h (MW cutoff = 6000−8000) to yield stable suspensions of mPEG−DTC coated nanorods with minimal CTAB. A similar procedure for removing CTAB was used to prepare nanorods coated with bis(*p*-sulfonatophenyl)phenylphosphine (BSP), an anionic surfactant. It should be mentioned that dialysis of CTAB-coated nanorods without prior exposure to chemisorptive surfactants will result in flocculation and precipitation.

Adherent KB cells (a tumor cell line derived from oral epithelium) were treated with 100-μL aliquots of nanorod solutions in serum-free RPMI growth medium and maintained under standard cell growth conditions prior to examination. Nanorod uptake under these conditions is presumed to be driven by the action of CTAB on the cell membranes, rather than by endocytosis induced by serum proteins adsorbed on the nanoparticle surface.[17] Nanorod uptake was monitored with a scanning laser microscope using two-photon luminescence (TPL), a nonlinear optical process which provides real-time imaging of biological samples with three-dimensional spatial resolution.[7] We recently demonstrated that gold nanorods can produce TPL under resonance conditions with sufficient brightness that they can be imaged with single-particle sensitivity,[2] enabling their use as TPL contrast agents for studying intracellular processes. Cells were washed with fresh RPMI growth medium to remove free nanorods prior to TPL imaging, which was performed on an inverted microscope with a 60× water objective (N.A. = 1.2). A femtosecond Ti:sapphire oscillator operating at 77 MHz was tuned to 795 nm for optimal two-photon excitation, and an incident power of 1−2 mW was used to minimize photothermal damage to the cells or the nanorods.

Results and Discussion

The CTAB-coated nanorods were internalized by KB cells at a high number density within a matter of hours and migrated toward the perinuclear region over a 24-h period. TPL images obtained at different focal depths confirmed that the majority of the nanorods were internalized rather than adsorbed on the cell membrane exterior (Figure 2a−c). The intensities of the peaks in a linescan of Figure 2b illustrates the high signal-to-background ratio of the TPL contrast produced by nanorods within the KB cells (Figure 2d). Although we have previously shown that TPL signals can be detected at the single-particle limit, we could not ascertain in this study whether any of the signals are represented by individual nanorods, as their intensities depend strongly on orientation with respect to the incident polarization.[2]

Single-particle tracking (SPT) analysis was conducted to determine the velocity and trajectory of the internalized nanorods (see Figure 3).[25] The nanorods clearly exhibited bidirectional motion over a 60-s interval, traveling alternately in the direction of the nucleus (positive trajectory) or toward the cell membrane (negative trajectory). The mean-squared displacement of the nanorods contains a quadratic time-dependent term consistent with directed motion (Figure 3d),[25] with an average velocity of 23 nm/s toward the nucleus and a diffusion rate of 420 nm^2/s. Vesicular transport of the nanorods is likely, as the activity of CTAB is expected to be similar to that of cationic transfection agents used in intracellular nanoparticle delivery.[1d,26] We have

(19) Sau, T. K.; Murphy, C. J. *Langmuir* **2004**, *20*, 6414−6420.
(20) Zweifel, D. A.; Wei, A. *Chem. Mater.* **2005**, *17*, 4256−4261.
(21) Berr, S. S. *J. Phys. Chem.* **1987**, *91*, 4760−4765.
(22) (a) Cortesi, R.; Esposito, E.; Menegatti, E.; Gambari, R.; Nastruzzi, C. *Int. J. Pharm.* **1996**, *139*, 69−78. (b) Mirska, D.; Schirmer, K.; Funari, S.; Langner, A.; Dobner, B.; Brezesinski, G. *Colloids Surf., B* **2005**, *40*, 51−59.
(23) Zhao, Y.; Pérez-Segarra, W.; Shi, Q.; Wei, A. *J. Am. Chem. Soc.* **2005**, *127*, 7328−7329.
(24) (a) Balasubramanian, R.; Kim, B.; Tripp, S. L.; Wang, X.; Lieberman, M.; Wei, A. *Langmuir* **2002**, *18*, 3676−3681. (b) Kim, B.; Carignano, M. A.; Tripp, S. L.; Wei, A. *Langmuir* **2004**, *20*, 9360−9365.
(25) Saxton, M. J.; Jacobson, K. *Annu. Rev. Biophys. Biomol. Struct.* **1997**, *26*, 373−399.
(26) Derfus, A. M.; Chan, W. C. W.; Bhatia, S. N. *Adv. Mater.* **2004**, *16*, 961−966.

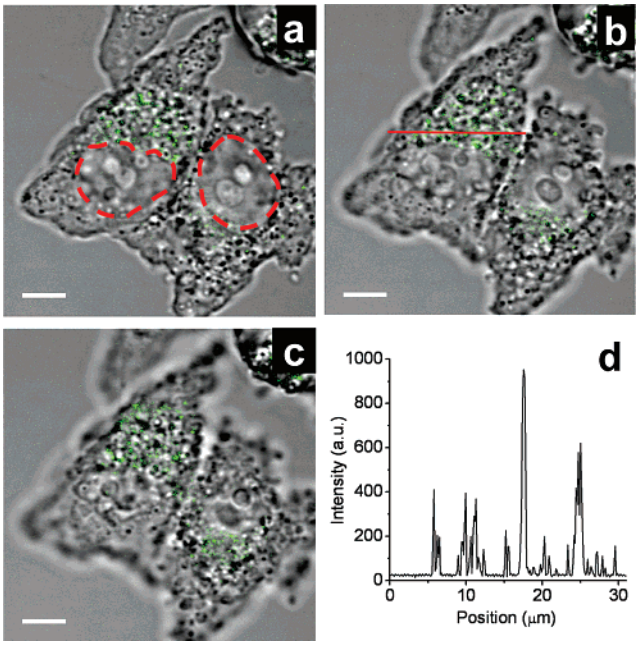

Figure 2. TPL images of KB cells with internalized gold nanorods (green), at three different focal depths. Positions of nuclei are outlined by red dashes for clarity. (a) $Z = 1.6$ μm; (b) $Z = 3.0$ μm; (c) $Z = 4.0$ μm. (d) Intensity profile across red line in (b). Bar = 10 μm.

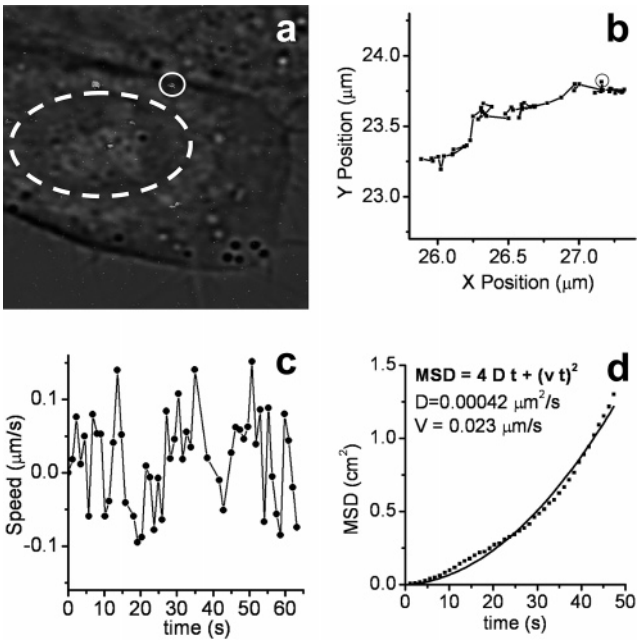

Figure 3. (a) Overlay of transmission and TPL images of nanorods inside KB cell. Solid circle highlights TPL signal being tracked; broken circle outlines the cell nucleus. (b) Nanorod trajectory through KB cell over a 60-s period (circle indicates starting position). (c) Nanorod velocity over a 60-s period. Positive values indicate motion in the direction of the cell nucleus; negative values indicate motion toward the cell membrane. (d) Mean-squared displacement (MSD) of nanorod signal, and a regressive curve fit describing active transport according to the function MSD = $4Dt + (Vt)^2$. $D = 420$ nm^2/s; $V = 23$ nm/s.

recently observed that bidirectional motion of the intracellular TPL signals is disrupted upon introduction of colchicine, which suggests that the transport of nanorods is directed along microtubules.[27]

(27) Tong, L.; Zhao, Y.; Huff, T. B.; Hansen, M. H.; Wei, A.; Cheng, J.-X. Manuscript in preparation.

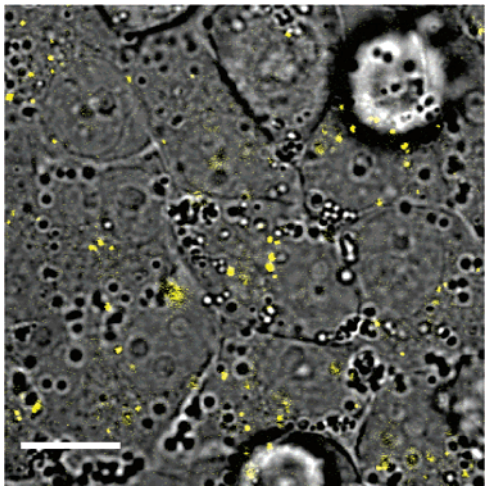

Figure 4. TPL image of CTAB-coated gold nanorods (yellow) internalized by KB cells, following 5 days of incubation. Bar = 20 μm.

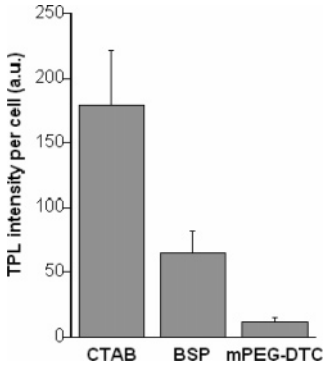

Figure 5. Mean TPL intensities from KB cells ($N = 90$) exposed to nanorods with different surfactant coatings, following a 24-h incubation period. TPL intensities per cell were corrected by subtracting background signals from areas of equal size. The level of nonspecific cell uptake of CTAB-coated nanorods is nearly 20 times greater than that of nanorods coated with mPEG−DTC.

KB cells with internalized CTAB-coated nanorods were monitored over 5 days for nanorod excretion or degradation, as well as for signs of cytotoxicity via changes in cell morphologies or behavior (see Figure 4). The cells were apparently unaffected by the internalized nanorods and grew to confluence over the 5-day period, in accord with other recent studies involving CTAB-coated nanoparticles.[15,16] With respect to the nanorods over this same period, the intracellular TPL signals were reduced in number but increased in brightness, and no extracellular TPL signals could be detected. This indicates that the internalized nanorods were not excreted by KB cells, but rather compartmentalized as aggregates.

To determine whether nonspecific nanorod uptake could be prevented by exchanging CTAB with hydrophilic surfactants such as BSP or mPEG−DTC, nanorods were treated with aqueous solutions of these chemisorptive compounds to displace CTAB from the nanorod surface, followed by membrane dialysis to remove the residual CTAB. Nanorods with different coatings were then incubated in a serum-free medium with KB cells, which were carefully washed after a 24-h period. TPL image analysis revealed that nanorods coated with BSP and mPEG−DTC were internalized at reduced levels compared with CTAB-coated nanorods (see Figure 5). In particular, the uptake of mPEG−DTC-conjugated nanorods was observed to be only 6% relative to that of the untreated nanorods.

The accumulation of nanorods in cells has a dual consequence for biomedical applications. On one hand, nanorods can serve as multifunctional imaging and therapeutic agents if selectively targeted for adsorption by tumor cells.[5,28] On the other hand, the nonspecific uptake of nanorods can produce interference during site-directed imaging or may inflict concurrent damage on healthy cells and tissues if photothermal treatments are applied. Applications involving the targeted delivery of nanorods should therefore ensure the complete removal of CTAB to safeguard against nonspecific uptake and accumulation. Conjugation of mPEG chains onto nanorod surfaces by in situ dithiocarbamate formation appears to be effective at maintaining stable nanorod dispersions in the absence of CTAB and can be expected to be compatible with established bioconjugation techniques.[29]

Acknowledgment. The authors gratefully acknowledge financial support from the National Institutes of Health (EB-001777-01), the National Science Foundation (CHE-0243496, ECS-0210445), Purdue Research Foundation, and a grant from the Oncological Sciences Center at Purdue University. KB cells were kindly provided by Prof. Phil Low. The authors thank Hongtao Chen for his kind assistance in the intracellular particle trafficking experiment.

LA062642R

(28) Huff, T. B.; Tong, L.; Zhao, Y.; Hansen, M. H.; Cheng, J.-X.; Wei, A. *Nanomedicine*, in press.

(29) Liao, H.; Hafner, J. H. *Chem. Mater.* **2005**, *17*, 4636−4641.